High-Coverage Oxygen Structures on Rh(111): Adsorbate Repulsion and Site Preference Is Not Enough

L. Köhler,[1] G. Kresse,[1] M. Schmid,[2] E. Lundgren,[3] J. Gustafson,[3] A. Mikkelsen,[3] M. Borg,[3] J. Yuhara,[4] J. N. Andersen,[3]
M. Marsman,[1] and P. Varga[2]

[1]*Institut für Materialphysik and Centre for Computational Materials Science, Universität Wien, A-1090 Wien, Austria*
[2]*Institut für Allgemeine Physik, Technische Universität Wien, A-1040 Wien, Austria*
[3]*Department of Synchrotron Radiation Research, Lund University, Box 118, S-221 00, Sweden*
[4]*Department of Physical Science and Engineering, Nagoya University, Nagoya, 464-8603, Japan*

(Received 21 June 2004; published 21 December 2004)

A new O induced structure on Rh(111) displaying a $(2\sqrt{3} \times 2\sqrt{3})R30°$ periodicity with an oxygen coverage of 2/3 has been studied by high resolution core level spectroscopy, scanning tunneling microscopy, and density functional theory. Although O favors fcc hollow sites in all other known phases, it occupies both fcc and hcp sites in this structure, which cannot be explained by pairwise adsorbate repulsion only. Both the $(2\sqrt{3} \times 2\sqrt{3})R30°$ and (2×2)-3O structures also exemplify that density-of-states contrast can lead to oxygen adatoms appearing as protrusions in scanning tunneling microscopy images.

DOI: 10.1103/PhysRevLett.93.266103 PACS numbers: 68.35.Bs, 68.37.Ef, 68.43.Bc, 68.47.Gh

The structures formed by adsorbates on surfaces are usually seen as a result of minimizing the energies of (i) -adsorbate-adsorbate interactions, which are usually considered to be pairwise and predominantly repulsive, and (ii) the site-dependent adsorption energy, which leads to a preference for a certain adsorption site already for a single isolated adsorbate. It has been noted previously that an exact description of adsorption energies needs complicated models including three-atom terms [1]. Nevertheless, for the determination of possible adatom structures the simple picture mentioned above is usually considered sufficient, at least as long as the substrate does not reconstruct [2]. Common adsorption systems studied are oxygen induced structures on metal substrates; one reason being the important role oxygen plays in catalytic reactions. Although it has been shown for some surfaces that it is not the chemisorbed O adatoms but rather oxides—bulk or ultrathin surface oxides [3–6]—that are the most efficient phase in oxidizing CO [7–9], chemisorbed O is still of considerable interest for catalysis. In fact, previous investigations have indicated that oxide formation on Rh(111) even poisons the adsorption of CO and thus hinders the CO oxidation reaction [10].

In the present Letter we present a structure not understandable using the simple pair-interaction outlined above, the $(2\sqrt{3} \times 2\sqrt{3})R30°$ oxygen superstructure on Rh(111). Using a combination of experimental and theoretical techniques we show that oxygen adsorbs in both fcc and hcp sites. We further demonstrate the existence of a $p(2 \times 2)$-3O superstructure with $\theta = 3/4$ monolayers (ML), and we show that the oxygen adatoms for these structures appear as protrusions in scanning tunneling microscopy (STM) images.

Previously, chemisorbed O on Rh(111) has been observed to form $p(2 \times 2)$ and $p(2 \times 1)$ structures with O coverages of $\theta = 1/4$ and $1/2$ ML, respectively. Low energy electron diffraction (LEED) [11], high-resolution core level spectroscopy (HRCLS) , and density functional theory (DFT) [13] have been used to study these structures and shown that the oxygen atoms reside in fcc hollow sites. Using molecular oxygen, or even by exposing the $p(2 \times 1)$ surface to NO [11] which is known to be strongly oxidizing, to our knowledge, no oxygen-on-surface structure with a coverage above $\theta = 1/2$ has been reported previously. However, using atomic O a $p(1 \times 1)$-O phase has been prepared [14].

For the present work, the HRCLS measurements were performed at beam line I311 at MAX II in Lund, Sweden [15]. A Donjiac-Šunjić profile [16] convoluted with a Gaussian distribution was used for the deconvolution of all spectra. STM measurements were done in Vienna at room temperature using the same instrument as in Refs. [4,6]. The cleaning procedure of the Rh(111) surface has been described elsewhere [6]. An oxygen induced $(2\sqrt{3} \times 2\sqrt{3})R30°$ structure could be formed by exposing the Rh(111) surface to 1×10^{-3} mbar of oxygen for 300 seconds at a sample temperature of 400 K or 550 K with cooldown to 400 K in oxygen. At the higher preparation temperatures, coexistence of the high-coverage adatom phases and the surface oxide [6] at the step edges was observed.

The density functional calculations were performed using the Vienna *ab initio* simulation package (VASP) [17], using the projector augmented wave method [18,19] and the generalized gradient approximation (GGA) [20]. The valence wave functions were expanded in a plane wave basis with a cutoff at 250 eV. With this setup, the lattice constant of Rh was determined to be $a_0 = 3.84$ Å, in excellent agreement with previous DFT-GGA calculations ($a_0 = 3.83$ Å, e.g., Ref. [13]). The Rh

© 2004 The American Physical Society

substrate was modeled by six layer thick slabs, and the Brillouin zone integration was performed with grids corresponding to 24×24 k-points in the primitive surface cell. Compared to our previous, less accurate setup [6] the average adsorption energies change by about 50 meV. The high computational accuracy was required since energy differences between different structures are tiny in the present case.

In Fig. 1 we show the O $1s$ and Rh $3d_{5/2}$ core level spectra of the $(2\sqrt{3} \times 2\sqrt{3})R30°$ structure and the LEED pattern. The Rh $3d_{5/2}$ level can be decomposed into four components. Apart from the bulk component at approximately 307.15 eV we find one component at lower binding energy and two at higher binding energies. Previously, for the $p(2 \times 1)$ structure, it has been shown that the lower binding energy component (-0.15 eV relative to the bulk component) is due to Rh atoms coordinated to one oxygen atom (1O), while the intermediate component shifted by about $+0.45$ eV is due to Rh atoms coordinated to two oxygen atoms (2O) [12]. When decomposing spectra taken with different excitation energies, it becomes clear that a fourth component with a shift of $+0.71$ eV must be included to obtain a consistent fit. One explanation for this component are Rh atoms coordinated to three O atoms. A second possibility, the presence of subsurface oxygen can be ruled out (see below). Turning to the O $1s$ spectra, we find that the O $1s$ emission can be described using only a single component. The component is broadened by approximately 0.2 eV as compared to the O $1s$ spectrum of the $p(2 \times 2)$ structure. Although a small shift or broadening does not necessarily point towards a single adsorption site, a comparison of the present spectra to the O $1s$ spectra of the (9×9) surface oxide—which involves oxygen atoms on top and below a Rh layer exhibiting a large binding energy shift [6]—suggests that subsurface oxygen can be excluded in the present case.

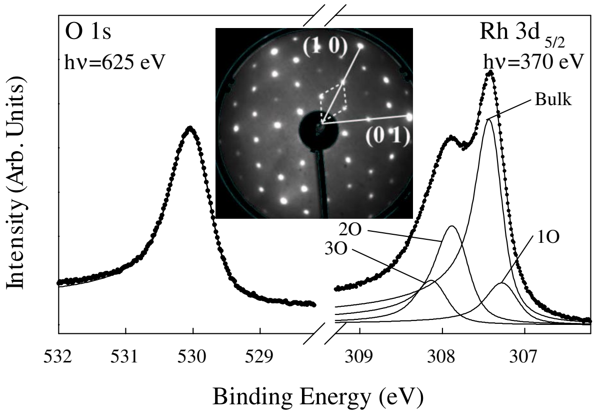

FIG. 1 (color online). HRCLS of the $(2\sqrt{3} \times 2\sqrt{3})R30°$ structure. The Rh$3d_{5/2}$ peak can be decomposed into four components with an O coordination of 1O, 2O, and 3O, whereas, the O $1s$ level exhibits only one component indicating no subsurface or oxide formation. (Inset) LEED pattern of the $(2\sqrt{3} \times 2\sqrt{3})R30°$ structure (electron energy 126 eV).

The oxygen coverage of the $(2\sqrt{3} \times 2\sqrt{3})R30°$ structure is consistent with both $\theta = 2/3$ or $\theta = 3/4$ ML, as obtained by comparing the O $1s$ spectra with those from the $p(2 \times 2)$ and $p(2 \times 1)$ structures. The uncertainty in the O coverage is mainly due to the coexistence of $(2\sqrt{3} \times 2\sqrt{3})R30°$ and $p(2 \times 2)$-3O domains with a local coverage of $\theta = 3/4$ ML.

Useful information about the relative abundance of different oxygen coordinated Rh atoms can be obtained by comparing the relative intensity of the different components in the Rh $3d_{5/2}$ spectra. Using the line shapes obtained for the $p(2 \times 2)$ and $p(2 \times 1)$ structures, we estimate that the ratios of Rh atoms binding to one, two, and three oxygen atoms are 1O:2O:3O $\approx$ 1:2:1.

In Fig. 2(a) we show an STM image of the coexisting $(2\sqrt{3} \times 2\sqrt{3})R30°$ and (2×2)-3O structures, and Fig. 2(c) shows a high-resolution Fourier filtered image of a $(2\sqrt{3} \times 2\sqrt{3})R30°$ domain. First, we have tried to analyze the structure using the usual assumption of the oxygen atoms and/or their metal neighbors appearing as depressions (dark) in STM [21]. It turned out that this attempt does not lead to any structure model with oxygen atoms in hollow or bridge sites and a reasonable O coverage unless large displacements of the Rh atoms and unrealistic Rh-Rh distances are assumed. Assuming that the oxygen atoms appear as protrusions (bright), the construction of a structure model is straightforward [Fig. 2(d)]. We find an O coverage of $\theta = 2/3$, with two O atoms per cell in hcp sites and six in fcc sites. The number of Rh atoms binding to one, two, and three O atoms are three, six and three, respectively, in perfect agreement with the HRCLS data, and the different environment of the O atoms in the structure explains the slight broadening of the O core level peak. The reproducibility of the STM image and the fact that similar images were obtained in a large range of tip-sample distances (tunneling voltages between -4 mV and -1.2 V) indicate that oxygen adatoms on Rh can appear as protrusions without a special tip or tip-sample interaction, as opposed to cases when oxygen atoms occasionally appeared as protrusions [22,23].

The $p(2 \times 2)$-3O structure also visible in Fig. 2(a) can be easily understood, if the oxygen atoms are also imaged as protrusions. By extrapolating the lattice from the $(2\sqrt{3} \times 2\sqrt{3})R30°$ into the $p(2 \times 2)$-3O domains we can determine that the protrusions are in three of the four fcc hollow sites of the $p(2 \times 2)$ cell. We find that the $p(2 \times 2)$-3O areas appear blurred in many parts of the image, indicating a high mobility of domain boundaries at room temperature.

The DFT calculations confirm the above model for the $(2\sqrt{3} \times 2\sqrt{3})R30°$ structure and furthermore verify that O atoms appear as bright protrusions in the STM image. The STM image, simulated using the simple Tersoff-Hamann approach [24] [Fig. 2(b)], resembles the experi-

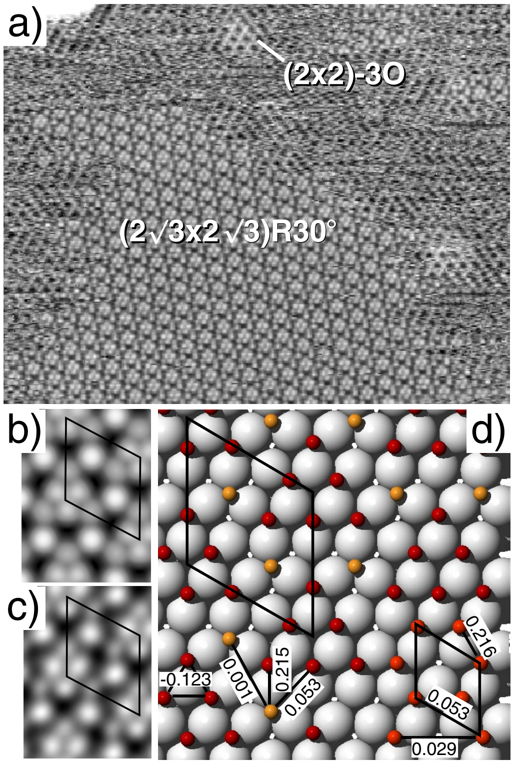

FIG. 2 (color online). (a) STM image of the $(2\sqrt{3}\times 2\sqrt{3})R30^\circ$ and $p(2\times 2)$-3O phase (20 nm wide; -95 mV, 0.46 nA). (b) Simulated STM image of the relaxed structure as obtained by DFT shown in (d). (c) Fourier filtered STM image of the $(2\sqrt{3}\times 2\sqrt{3})R30^\circ$ to be compared to (b). (d) Structure as obtained by DFT. Small balls are O atoms, dark in fcc sites, lighter in hcp sites. In the lower right corner the honeycomb $(\sqrt{3}\times\sqrt{3})R30^\circ$-2O structure is illustrated. Interaction energies for O pairs and an O_3 triangle are also indicated.

mental image in Fig. 2(c) to such a degree that few doubts concerning the correctness of the model remain. In the Tersoff-Hamann approach the protrusions are bias independent between ± 1 V and related to a charge accumulation at the Fermi-level on top of the oxygen atoms. Additional proof stems from calculated core level shifts of the Rh surface atoms, as well as from the binding energy shifts of the O 1*s* levels. For the $(2\sqrt{3}\times 2\sqrt{3})R30^\circ$ structure, binding energy shifts of -0.16 eV, 0.43 eV, and 0.56 eV are calculated for the Rh atoms coordinated to one, two, and three oxygens atoms, respectively. This is in excellent agreement with the experimental values for the 1O (-0.15 eV), 2O (0.45 eV), and in reasonable agreement for the 3O (0.71 eV) component. The calculated O 1*s* binding energies vary by 0.15 eV in good agreement with the experimentally observed broadening of the O 1*s* spectra by 0.2 eV. The binding energies are smallest for the oxygen atoms in the hcp site, and largest for the oxygen atoms at the sides of the triangles formed by six O atoms.

Figure 3 shows the calculated surface phase diagram, including the previously determined ultrathin Moiré O-Rh-O oxide phase [6]. First of all, it is obvious that both the $(2\sqrt{3}\times 2\sqrt{3})R30^\circ$ and the (2×2)-3O phases are only kinetically stabilized phases, since both the O-Rh-O(8×8)@Rh(9×9) surface oxide and the Rh_2O_3 bulk phase are lower in energy at the oxygen rich side of the phase diagram. Formation of the surface and bulk oxides, however, is kinetically hindered and occurs only at higher temperatures around 800 K (and higher pressures) as discussed in our previous work [6]. Considering only adatom structures and no (surface) oxides, the $(2\sqrt{3}\times 2\sqrt{3})R30^\circ$ structure is stable between a chemical potential of -1.07 and -0.64 eV, corresponding to temperatures of 400–700 K at a pressure of 1×10^{-3} mbar. This agrees quantitatively with the experimental preparation conditions.

To disentangle the stability of the $(2\sqrt{3}\times 2\sqrt{3})R30^\circ$ phase, pair and triple interaction parameters were determined using a (4×4) supercell. The repulsive pairwise interaction energies are summarized in Fig. 2(d). A significant triple interaction energy was only found for three oxygen atoms arranged in a triangle (the triangle is 0.123 eV more stable than predicted by the additive pairwise repulsion), whereas, for other arrangements the trio interaction energies are small. Table I shows that the interaction parameters can be used to predict the average oxygen adsorption energies with an accuracy of roughly 20 meV (with the exception of the (2×2)-3O phase, see below).

In particular, we have to discuss why the $(2\sqrt{3}\times 2\sqrt{3})R30^\circ$-8O is more stable than an alternative 2/3 ML structure with a honeycomb $(\sqrt{3}\times\sqrt{3})R30^\circ$-2O arrangement of oxygen atoms in fcc sites [lower right corner in Fig. 2(d)]. In GGA this arrangement is less stable by 80 meV per oxygen atom than the experimen-

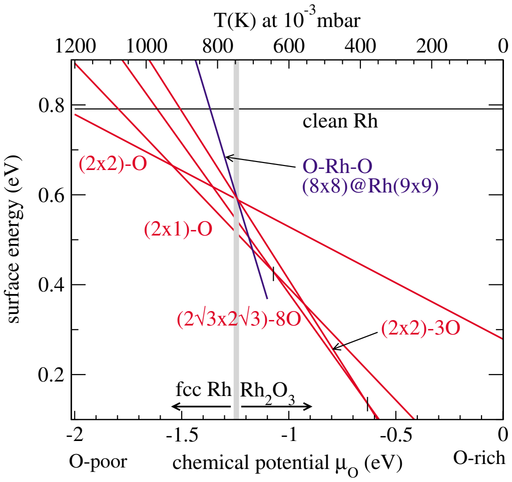

FIG. 3 (color online). Calculated phase diagram for oxygen-on Rh(111). The chemical potential can be related to the temperature and the oxygen partial pressure [28]. The stability regime of the $(2\sqrt{3}\times 2\sqrt{3})R30^\circ$ phase is indicated by small ticks.

TABLE I. Average oxygen adsorption energy (in eV) for a number of structures as calculated by GGA and predicted using the pair and triple interaction energies indicated in Fig. 2(d).

	GGA	Pair + Triple
$(4 \times 4) - \mathrm{O}$ (fcc)	−2.114	
$(4 \times 4) - \mathrm{O}$ (hcp)	−2.013	
$(2 \times 2) - \mathrm{O}$	−2.051	−2.030
$(2 \times 1) - \mathrm{O}$	−1.795	−1.762
$(2\sqrt{3} \times 2\sqrt{3})R30°\text{-}8\mathrm{O}$	−1.614	−1.637
$(\sqrt{3} \times \sqrt{3})R30°\text{-}2\mathrm{O}$	−1.530	−1.547
$(2 \times 2) - 3\mathrm{O}$	−1.506	−1.576

tally observed structure. The crucial result is that the $(2\sqrt{3} \times 2\sqrt{3})R30°$-8O is stabilized by the attractive triple interaction energy, which itself is caused by an outwards relaxation of the oxygen atoms at the corners of the triangles towards the bridge sites. This relaxation occurs for a triangular arrangement of three and six oxygen atoms. If the oxygen atoms are kept exactly above the fcc hollow site, the $(2\sqrt{3} \times 2\sqrt{3})R30°$-8O structure is calculated to be degenerate with the $(\sqrt{3} \times \sqrt{3})R30°$-2O phase (−1.534 eV). It is now also apparent why the predictions for the (2×2)-3O phase are wrong if the triplet interaction parameters are included. In this phase, the oxygen atoms can not relax towards the bridge site and, hence, the energy without triple interaction parameters (−1.494 eV) agrees much better with the calculated GGA value of −1.506 eV.

These results imply that several factors are important for the realization of the hcp site on Rh(111): (i) the small energy difference between the fcc and hcp sites is a prerequisite, (ii) relaxation towards bridge sites allows a significant reduction of the repulsion between oxygen atoms in the triangles, and (iii) the empty space in between the triangles can accommodate two oxygen adatoms in hcp sites that experience only a relatively weak repulsion to neighboring O atoms. The correct structure model cannot be found by reasoning based on simple repulsive nearest neighbor interactions between oxygen atoms, because in the $(2\sqrt{3} \times 2\sqrt{3})R30°$-8O the average number of fcc-fcc and hcp-fcc nearest neighbors is 3.75, whereas, it is only three in the $(\sqrt{3} \times \sqrt{3})R30°$-2O structure. Furthermore, in the present case, the trio interaction parameters must include relaxation effects, which hitherto have not been included [1]. In any case, it is remarkable to find a coexistence of oxygen adsorbed in hcp and fcc sites in the $(2\sqrt{3} \times 2\sqrt{3})R30°$ structure, whereas, in all previous studies the adsorption site of atomic oxygen on fcc(111) surfaces was the fcc site. To our knowledge, a related observation has only been reported in the case of the O/Ni(111) system in which $p(2 \times 2)$ domains with oxygen adsorbed in fcc sites are separated by domain walls in which hcp sites are occupied [25,26].

A second key observation of the present study is that oxygen atoms appear in STM as protrusions on Rh(111) at higher coverage in both the $(2\sqrt{3} \times 2\sqrt{3})R30°$ and the $p(2 \times 2)$-3O structures. This contradicts the common assertion that oxygen atoms are imaged as depressions in experimental STM images (see also Ref. [27]). It is emphasized that the bright appearance of oxygen atoms is not related to a special tip or special tip-substrate interaction in the present case. This observation implies that STM images must be interpreted with considerable caution when oxygen is involved.

This work was financially supported by the Austrian *Fonds zur Förderung der wissenschaftlichen Forschung*, the Swedish Research Council, and the European Union under Contract No. NMP3-CT-2003-505670 (NANO2). Support by the MAX-lab staff is gratefully acknowledged. The computations were performed on Schrödinger II at the computing center of the University of Vienna.

[1] C. Stampfl, H. J. Kreuzer, S. H. Payne, H. Pfnür, and M. Scheffler, Phys. Rev. Lett. **83**, 2993 (1999).
[2] G. A. Samorjai, *Introduction to Surface Chemistry and Catalysis* (J. Wiley and Sons, New York, 1994).
[3] C. I. Carlisle, D. A. King, M.-L. Bocquet, J. Cerdá, and P. Sautet, Phys. Rev. Lett. **84**, 3899 (2000).
[4] E. Lundgren *et al.*, Phys. Rev. Lett. **88**, 246103 (2002).
[5] M. Todorova *et al.*, Surf. Sci. **541**, 101 (2003).
[6] J. Gustafson *et al.*, Phys. Rev. Lett. **92**, 126102 (2004).
[7] H. Over *et al.*, Science **287**, 1474 (2000).
[8] B. L. M. Hendriksen and J.W. M. Frenken, Phys. Rev. Lett. **89**, 046101 (2002).
[9] B. L. M. Hendriksen and J.W. M. Frenken, Surf. Sci. **552**, 229 (2004).
[10] C. H. F. Peden *et al.*, J. Phys. Chem. **92**, 1563 (1988).
[11] S. Schwegmann *et al.*, Surf. Sci. **375**, 91 (1997).
[12] M.V. Ganduglia-Pirovano *et al.*, Phys. Rev. B **63**, 205415 (2001).
[13] M.V. Ganduglia-Pirovano and M. Scheffler, Phys. Rev. B **59**, 15533 (1999).
[14] K. D. Gibson *et al.*, J. Chem. Phys. **110**, 2757 (1999).
[15] R. Nyholm *et al.*, Nucl. Instrum. Methods Phys. Res., Sect. A **467**, 520 (2001).
[16] S. Donjiac and M. Šunjić, J. Phys. C **3**, 285 (1970).
[17] G. Kresse and J. Furthmüller, Comput. Mater. Sci. **6**, 15 (1996).
[18] G. Kresse and D. Joubert, Phys. Rev. B **59**, 1758 (1998).
[19] P. E. Blöchl, Phys. Rev. B **50**, 17953 (1994).
[20] J. P. Perdew *et al.*, Phys. Rev. B **46**, 6671 (1992).
[21] P. Sautet, Surf. Sci. **374**, 406 (1997).
[22] L. Ruan, F. Besenbacher, I. Stensgaard, and E. Laegsgaard, Phys. Rev. Lett. **70**, 4079 (1993).
[23] M. Sporn *et al.*, Surf. Sci. **416**, 384 (1998).
[24] J. Tersoff and D. R. Hamann, Phys. Rev. B **31**, 805 (1985).
[25] C. Schwennicke and H. Pfnür, Surf. Sci. **369**, 248 (1996).
[26] D. Kolthoff, C. Schwennicke, and H. Pfnür, Surf. Sci. **529**, 443 (2003).
[27] F. Calleja *et al.*, Phys. Rev. Lett. **92**, 206101 (2004).
[28] K. Reuter and M. Scheffler, Phys. Rev. B **65**, 035406 (2002).